Ultramicroscopy ∎ (∎∎∎∎) ∎∎∎–∎∎∎

Contents lists available at ScienceDirect

Ultramicroscopy

journal homepage: www.elsevier.com/locate/ultramic

Full length article

Strong excitonic interactions in the oxygen K-edge of perovskite oxides

Kota Tomita [a], Tomohiro Miyata [a], Weine Olovsson [b], Teruyasu Mizoguchi [a,*]

[a] Institute of Industrial Science, The University of Tokyo, 4-6-1 Komaba, Meguro, Tokyo 153-8505, Japan
[b] Department of Physics, Chemistry and Biology (IFM), Linköping University, SE-581 83 Linköping, Sweden

ARTICLE INFO

Article history:
Received 18 January 2016
Received in revised form
30 March 2016
Accepted 12 April 2016

Keywords:
Electron energy-loss near-edge structure
First principles calculation
Exciton
Perovskite oxides
Oxygen K-edge

ABSTRACT

Excitonic interactions of the oxygen K-edge electron energy-loss near-edge structure (ELNES) of perovskite oxides, $CaTiO_3$, $SrTiO_3$, and $BaTiO_3$, together with reference oxides, MgO, CaO, SrO, BaO, and TiO_2, were investigated using a *first-principles* Bethe–Salpeter equation calculation. Although the transition energy of oxygen K-edge is high, strong excitonic interactions were present in the oxygen K-edge ELNES of the perovskite oxides, whereas the excitonic interactions were negligible in the oxygen K-edge ELNES of the reference compounds. Detailed investigation of the electronic structure suggests that the strong excitonic interaction in the oxygen K-edge ELNES of the perovskite oxides is caused by the directionally confined, low-dimensional electronic structure at the Ti–O–Ti bonds.

1. Introduction

The advanced aberration correction and monochromator systems for the transmission electron microscope make it possible to obtain electron energy-loss near-edge structure (ELNES) with high spatial and energy resolution. Electron transitions from a core orbital to unoccupied bands give rise to ELNES, thus, the spectral feature reflects the partial density of states (PDOS) of the atom under investigation [1]. ELNES observed with modern equipment offers the potential to detect the local atomic structure and the chemical states of materials at atomic resolution [2–6].

Theoretical methods for calculating ELNES have advanced in parallel with the development of experimental facilities. ELNES calculations can be categorized into three theoretical frameworks: the one-particle method, the two-particle method and the multi-particle method. In the one-particle method, particle–particle interactions are approximated as interactions between an electron and the mean field generated by other particles. The one-particle calculation is based on density functional theory (DFT) within the local density approximation (LDA) or generalized gradient approximation (GGA) [7–10]. The two-particle calculation considers the two-particle interaction between an excited electron and an electronic hole, i.e., core excitons. To include core–exciton effects, the two-particle formalism employs the Bethe–Salpeter equation (BSE) [11–15]. The multi-particle method calculates interactions between multi-particles, including electron–electron and electron–hole interactions, using, for example, the configuration interaction method [16–19]. It is known that the two-particle interaction is significant in low-energy ELNES (energies lower than 100 eV), and the multi-particle calculation is necessary for calculating the $L_{2,3}$-edge of transition metals and the $M_{4,5}$-edge of lanthanide, i.e., white lines. The DFT–LDA/GGA calculation is applicable for other cases, such as metal K-edges and anion K-edges.

However, an important open question is still present in the ELNES calculation. That is, the effect of the excitonic interaction at high-energy ELNES is not sufficiently discussed. The exciton in the ELNES is a core exciton between the excited electron and the core hole. The excitonic interaction is approximated using the DFT–LDA/GGA framework in the one-particle calculation. If the energy distance between the electron and hole is large, such as the case in high-energy ELNES, the one-particle approximation works well. The excitonic interaction in the high-energy ELNES (O K-edge at 530 eV and Mg K-edge at 1310 eV in MgO) was investigated by Rehr et al. [20]. They concluded that the one-particle calculation gave the same spectrum as the two-particle calculation for those high-energy ELNES.

In semiconductor optics, on the other hand, it is known that exciton behavior is strongly dependent on the electronic structure of material. For example, excitonic interaction at the band gap, i.e., the “band gap”-exciton, is affected by the size of the band gap and band dispersion. Furthermore, it is known that low-dimensional materials show strong excitonic interaction because of their confined electronic structure [21]. Contrary to the band gap exciton, the possibility of the presence of a strong “core”–excitonic interaction in high-energy ELNES has not been discussed.

In this study, we employed the BSE calculation (two-particle calculation) to study the O K-edge of perovskite materials. The O

* Corresponding author.
E-mail address: teru@iis.u-tokyo.ac.jp (T. Mizoguchi).

http://dx.doi.org/10.1016/j.ultramic.2016.04.006
0304-3991/

K-edge is located near 530 eV and is known to have a weak excitonic interaction [20]. Previously, we observed fine structures that could not be reproduced using the one-particle calculation [22]. In this study, the O K-edge of the perovskite oxides $CaTiO_3$, $SrTiO_3$, and $BaTiO_3$, and the reference oxides MgO, CaO, SrO, BaO, and TiO_2 were systematically calculated using both BSE (two-particle calculation) and DFT–GGA (one-particle calculation). The results are compared and the origin of the excitonic interaction in the O-K edge is discussed.

2. Methods

The first-principles full-potential linearized augmented plane-wave method based on DFT–GGA, as implemented in the Elk code, was used in this study [23]. The Perdew–Burke–Ernzerhof GGA was used to approximate the exchange correlation term [24]. In the one-particle calculation, one core hole was introduced into the oxygen 1s orbital. To minimize the artificial interactions between core holes, a large supercell was used. We employed 135-atom supercells for cubic $CaTiO_3$, $SrTiO_3$ and $BaTiO_3$, 128-atom supercells for MgO, CaO, SrO and BaO, and a 108-atom supercell for TiO_2 (anatase). For these supercells, the distance between core holes was greater than 10 Å, which is known to be large enough to reduce the artificial interaction [25–27]. The theoretical transition probability was calculated using the Fermi's golden rule.

In the two-particle (excitonic) calculation, the excitonic interaction was calculated using the BSE, in which the equation of the motion for the electron–hole pair was solved using the two-particle Green's function. The ground state calculation was performed by excluding the Coulomb interaction between the excited electron and the core-hole, namely random-phase approximation (RPA). In the BSE calculation, 125 k-points were used and the range of included conduction states was 30 for all compounds. A Gaussian broadening of 0.5 eV at full-width at half-maximum was applied to the calculated spectra to allow comparison with experimental spectra.

For simplicity, the one-particle calculation and the two-particle (excitonic) calculation are hereafter referred to as GGA and BSE, respectively.

3. Results

Fig. 1 shows experimental and calculated oxygen K-edge of MgO. In accordance with the previous reports, both GGA and BSE were able to reproduce the experimental spectrum [20,28] Fig. 2 compares the experimental oxygen K-edge spectrum for $CaTiO_3$ [29] with the GGA and BSE calculated spectra. The experimental spectrum comprises sharp peak A, which is followed by broad peak B, a distinct peak C, and small shoulder D. To investigate the fine features in detail, the experimental and calculated spectra were aligned using peak C, indicated by arrows in Fig. 2. To facilitate identification of the origin of each peak, the PDOS diagram is shown in Fig. 3. The PDOS diagram was calculated using GGA employing the primitive cell at the ground state. The GGA calculation reproduces the characteristic features of the experimental spectrum (Fig. 2) and peaks A and B originate from the O p-orbital hybridized with the Ti d-orbital (Fig. 3). Because Ti has six-fold octahedral symmetry, peaks A and B can be ascribed to the hybridized peak with Ti-d t_{2g}-and e_g-type components, respectively. Peaks C and D come from the O p-orbital hybridized with the Ca d-orbital. Because Ca is coordinated by 12 oxygens with O_h point symmetry, peaks C and D can be ascribed to hybridized peaks with Ca-d e_g-and t_{2g}-type components, respectively.

Detailed investigation of the peaks highlighted several discrepancies between the experimental spectrum and the spectrum

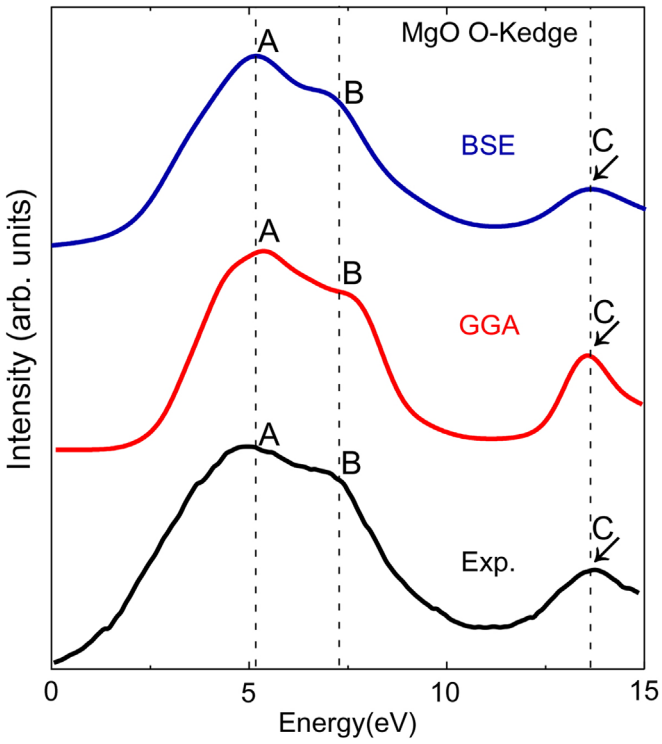

Fig. 1. Calculated and experimental [28] oxygen K-edge of MgO.

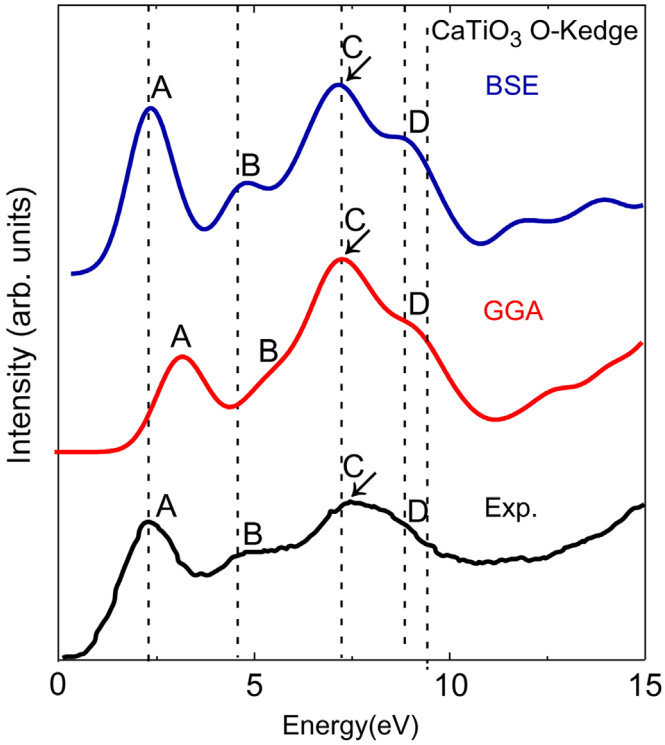

Fig. 2. Calculated and experimental [29] oxygen K-edge of $CaTiO_3$. Spectra were aligned using peak C, indicated by arrows.

calculated using GGA. The distance between peaks A and C in the experimental spectrum was 5.2 eV, whereas it was 4.1 eV in the spectrum calculated using GGA, i.e., a 1.1 eV error is present in the GGA calculation. Furthermore, peak B is less intense in the GGA calculation than the experimental spectrum. Conversely, the BSE calculation reproduces the A–C peak distance and small peak B well. This result suggests that, contrary to the case of MgO (Fig. 1),

Please cite this article as: K. Tomita, et al., Strong excitonic interactions in the oxygen K-edge of perovskite oxides, Ultramicroscopy (2016), http://dx.doi.org/10.1016/j.ultramic.2016.04.006